Journal of Marine Systems 186 (2018) 85–95

Contents lists available at ScienceDirect

Journal of Marine Systems

journal homepage: www.elsevier.com/locate/jmarsys

Development of under-ice stratification in Himmerfjärden bay, North-Western Baltic proper, and their effect on the phytoplankton spring bloom

Elina Kari[a], Ioanna Merkouriadi[b], Jakob Walve[a], Matti Leppäranta[c], Susanne Kratzer[a,*]

[a] Department of Ecology, Environment and Plant Sciences, Stockholm University, Sweden
[b] Norwegian Polar Institute, Norway
[c] Institute of Atmospheric and Earth Sciences, University of Helsinki, Finland

ARTICLE INFO

Keywords:
Seasonal sea ice
Under-ice plume
Stratification
Phytoplankton spring bloom
Onset
Phytoplankton composition
Baltic Sea

ABSTRACT

Seasonal sea ice cover reduces wind-driven mixing and allows for under-ice stratification to develop. These under-ice plumes are a common phenomenon in the seasonal sea ice zone. They stabilize stratification and concentrate terrestrial runoff in the top layer, transporting it further offshore than during ice-free seasons. In this study, the effect of sea ice on spring stratification is investigated in Himmerfjärden bay in the NW Baltic Sea. Distinct under-ice plumes were detected during long ice seasons. The preconditions for the development of the under-ice plumes are described as well as the typical spatial and temporal dimensions of the resulting stratification patterns. Furthermore, the effect of the under-ice plume on the timing of the onset and the maximum of the phytoplankton spring bloom were investigated, in terms of chlorophyll-a (Chl-a) concentrations. At the head of the bay, bloom onset was delayed on average by 18 days in the event of an under-ice plume. However, neither the maximum concentration of Chl-a nor the timing of the Chl-a maximum were affected, implying that the growth period was shorter with a higher daily productivity. During this period from spring bloom onset to maximum Chl-a, the diatom biomass was higher and *Mesodinium rubrum* biomass was lower in years with under-ice plumes compared to years without under-ice plumes. Our results thus suggest that the projected shorter ice seasons in the future will reduce the probability of under-ice plume development, creating more dynamic spring bloom conditions. These dynamic conditions and the earlier onset of the spring bloom seem to favor the *M. rubrum* rather than diatoms.

1. Introduction

The Baltic Sea is a shallow intracontinental sea with a limited water exchange with the North Sea (e.g. Lehmann et al., 2002; Leppäranta and Myrberg, 2009). The water mass of the Baltic Sea is brackish, a mixture of saline seawater originating from the North Sea and freshwater from terrestrial runoff. Another characteristic of the Baltic Sea is the seasonal sea ice cover which varies substantially in duration, timing and extent (Leppäranta and Myrberg, 2009) depending on the large-scale atmospheric circulation and the following weather conditions during winter (Uotila et al., 2015). Ice cover hinders the wind-driven mixing, affects the heat exchange between the sea and the atmosphere, and reduces the sunlight penetrating into the sea - especially when snow has fallen onto the ice (Warren, 1982; Leppäranta, 2003; Uusikivi et al., 2006; Granskog et al., 2006; Leppäranta and Myrberg, 2009; Vihma and Haapala, 2009; Thomas and Dieckmann, 2010; Lei et al., 2011; Merkouriadi and Leppäranta, 2015). In the landfast ice zone, wind-driven mixing is notably reduced, providing conditions for under-ice stratification patterns to develop. Due to the high buoyancy of freshwater from terrestrial runoff, distinct freshwater plumes can form just below the ice cover, the so-called under-ice plumes (Granskog et al., 2005). These under-ice plumes are a common coastal phenomenon in water basins with seasonal sea ice cover and inflow from rivers and streams (Granskog et al., 2005; Merkouriadi and Leppäranta, 2014, 2015). The development and physical characteristics of under-ice plumes are fairly well understood (Granskog et al., 2005; Merkouriadi and Leppäranta, 2015). However, there are only few studies about their effects on coastal ecology, and specifically on the development of the phytoplankton spring bloom (Eilola and Stigebrandt, 1998; Spilling, 2007; Kremp et al., 2008).

The length of the ice season in the Baltic Sea varies usually between 4 and 7 months. Despite the high natural variability of the ice seasons, time series studies show a decrease in both the maximum ice extent and the length of the ice season (Jevrejeva et al., 2004; Vihma and Haapala, 2009; Haapala et al., 2015). Merkouriadi and Leppäranta (2014) showed a significant decrease of the ice season length, by 30 days

* Corresponding author.
E-mail address: Susanne.Kratzer@su.se (S. Kratzer).

https://doi.org/10.1016/j.jmarsys.2018.06.004
Received 22 December 2017; Received in revised form 18 June 2018; Accepted 18 June 2018
Available online 20 June 2018

during the last century in the western Gulf of Finland. Warming climate shortens the ice seasons in the Baltic Sea, therefore reducing the probability of under-ice plumes. As the ice conditions are undergoing such dramatic changes, it is important to understand the current role of sea ice for the Baltic Sea ecosystem. In this study, we investigate the preconditions for under-ice plume development in a Baltic Sea coastal bay, as well as the spatial and temporal dimensions of the stratification pattern. The freshwater runoff transports high contents of humic substances and suspended matter increasing concentrations of coloured dissolved organic matter (CDOM) and suspended particulate matter (SPM) in Baltic Sea coastal waters (Kratzer and Tett, 2009; Harvey et al., 2015; Kari et al., 2016). The under-ice plume enhances the horizontal transport of terrestrial runoff, including nutrients, CDOM, and other substances, further towards the open sea, due to reduced mixing (Granskog et al., 2005). Here, we develop a new empirical model to estimate CDOM absorption from surface salinity, in order to discuss the role of CDOM for the timing of the spring bloom onset during under-ice plumes.

Phytoplankton spring blooms are annual phenomena in the Baltic Sea (e.g. Höglander et al., 2004; Fleming and Kaitala, 2006; Kremp et al., 2008; Kahru et al., 2016). The onset, intensity, and duration of the blooms depend on the light and nutrient availability – factors interacting with the water column stratification (e.g. Kahru and Nõmmann, 1990; Wasmund et al., 1998; Kratzer et al., 2003; Höglander et al., 2004; Fleming and Kaitala, 2006; Winder et al., 2012; Klais et al., 2013). During winter, nutrients are abundant in Baltic Sea coastal waters and thus the onset of the phytoplankton spring bloom is controlled by the light availability and the water column stratification (Wasmund et al., 1998; Fleming and Kaitala, 2006; Klais et al., 2013). The light availability under snow-covered ice is insufficient for primary production, but changes drastically when the snow melts and more light can penetrate through the ice (e.g. Leppäranta, 2003). As soon as the light availability is sufficient within the mixing depth, the spring bloom is expected to initiate (Kahru and Nõmmann, 1990; Eilola and Stigebrandt, 1998; Wasmund et al., 1998). The significance and role of the under-ice plumes on the onset and composition of the phytoplankton spring bloom is yet to be studied. Under-ice plumes stabilize the stratification, offering a calm, but cold, environment for the phytoplankton within the euphotic zone.

During the spring bloom, the phytoplankton species of our study area (coastal north-western Baltic proper) mainly belong to the diatom and dinoflagellate groups, but the photosynthetic ciliate *Mesodinium rubrum* can also be abundant (Fleming and Kaitala, 2006; Spilling, 2007; Klais et al., 2011). Kremp et al. (2008) suggest that long-term climatic trends may affect the phytoplankton composition more than the actual nutrient conditions at the time of bloom onset. Phytoplankton species are generally very sensitive to hydrographic conditions, which in turn are often governed by the climate. There are indications that the phytoplankton composition during the spring bloom may shift from diatom to dinoflagellate dominance (Wasmund and Uhlig, 2003; Kremp et al., 2008; Klais et al., 2011). A possible shift in the species composition and dominance can have ecosystem-wide consequences by affecting the nutrient cycling in pelagic ecosystem (Kremp et al., 2008). In this study, we compare spring seasons with and without under-ice plumes. The aim is to describe and discuss the impact of ice cover on the stratification in a bay with relatively low freshwater input and to investigate if under-ice plumes influence the timing and phytoplankton composition of the spring bloom in the Baltic Sea.

2. Materials and methods

The study site, Himmerfjärden, is a frequently monitored bay, located in the southern Stockholm archipelago in the north-western Baltic proper (Fig. 1). Himmerfjärden is about 30 km long and rather shallow with a mean depth of about 17 m. The bay is affected by the effluents of a sewage treatment plant serving southern Stockholm, with the outlet located close to station H5. The water circulation within the bay is estuarine with a relatively low freshwater input from streams and from Lake Mälaren (Engqvist and Omstedt, 1992; Engqvist and Stenström, 2009). There are also several sills, restricting the water exchange with the open Baltic Sea. The surface water (0–10 m) retention time is about 20 days based on a mass-balance model for salt (Khalili, 2007; Håkanson and Stenström-Khalili, 2010), for the deep water the retention time is up to 140 days (Engqvist, 1996). The monitoring stations H6-H2 (Fig. 1), located within Himmerfjärden, are used here for studying the extent and effects of the under-ice plume and station B1, located outside Himmerfjärden, is used as a reference station.

Meteorological and hydrological data were provided by the Swedish Meteorological and Hydrological Institute (SMHI) open data portal. These included daily air temperature, precipitation, and wind speed from Landsort A and runoff at the Södertälje lock (see map, Fig. 1). These meteorological and hydrological quantities were studied from 1st January to 30th April in 1997–2015. Modeled accumulated global irradiance ($W\,h\,m^{-2}$) data are available since January 1999, provided by the STRÅNG model system and validated by SMHI (STRÅNG, 2017). We used the daily data for the time period 1999–2015, focusing on the spring season from 1st January to 30th April. The irradiance data was retrieved for station H4 to represent Himmerfjärden bay. The spatial resolution of the STRÅNG model was about 22 × 22 km in 1999–2006 and 11 km × 11 km in 2007–2015.

Sea ice data were retrieved from two data sources: ice charts from the Finnish Meteorological Institute (FMI) and Baltic Sea ice codes from the SMHI. The ice charts are compiled daily by ice analysts, based on multiple data sources: remote sensing data, model results, and in situ measurements. The SMHI Ice service provided the 'Baltic Sea Ice codes', which are also based on ice charts, for the period 1997 to 2015. This ice code is a four-digit code, describing the ice conditions, where the first digit represents the ice concentration, i.e. ice cover area in percent. The other digits describe the stage of ice development, topography of ice and navigation conditions in ice along the fairway. Here, we used the first digit for the fairway from Södertälje at the head of Himmerfjärden to Landsort in the open sea (see map, Fig. 1). The days with ice concentration greater than zero were summed up in order to calculate the number of ice days. The Baltic Sea ice code data was used in this study to determine the ice conditions at the monitoring stations.

Most water quality data were obtained from the research and environmental control program of the Himmerfjärden sewage treatment plant (H6-H2) and the Swedish national marine monitoring program (station B1). Here, the time period from January to May each year 1997–2015 was investigated with a focus on Conductivity-Temperature-Depth (CTD) -profiler data, chlorophyll-a concentration (Chl-a), and Secchi depth. These parameters are measured once a month from November to February, every second week in early March, and weekly from the end of March to mid-May at stations H6-H3 and B1. CTD-profiling data were used to evaluate the stratification conditions. Water density (unit: $kg\,m^{-3}$) was calculated from the conservative temperature and absolute salinity values (unit: $g\,kg^{-1}$, ppt, parts per thousand, in the following), based on the Thermodynamic Equation of Seawater 2010 (TEOS-10) (McDougall and Barker, 2011). Here, sigma-t values were used, i.e. $1000\,kg\,m^{-3}$ was subtracted from the water density. The vertical sigma-t profiles were interpolated along a transect in order to visualize the spatial stratification patterns and identify the under-ice plumes. The under-ice plume is a distinct layer of less dense water, reaching out from the head of the bay. Chl-a was sampled as vertically integrated samples of the upper 0–14 m at H6-H3 and 0–20 m at B1 using a plastic hose (2.5 cm inner diameter) equipped with a weight at the lower end and a valve at the upper end. Water from the hose was mixed in a bucket and 1–2 l filtered on 47 mm GF/F glass fiber filters and stored frozen until extraction with acetone and absorbance measurement on a Hitachi U-2000 spectrophotometer (Swedish standard method SS028146). During ice cover, the Secchi depth was measured on board ship in the channel that was broken by the ship into

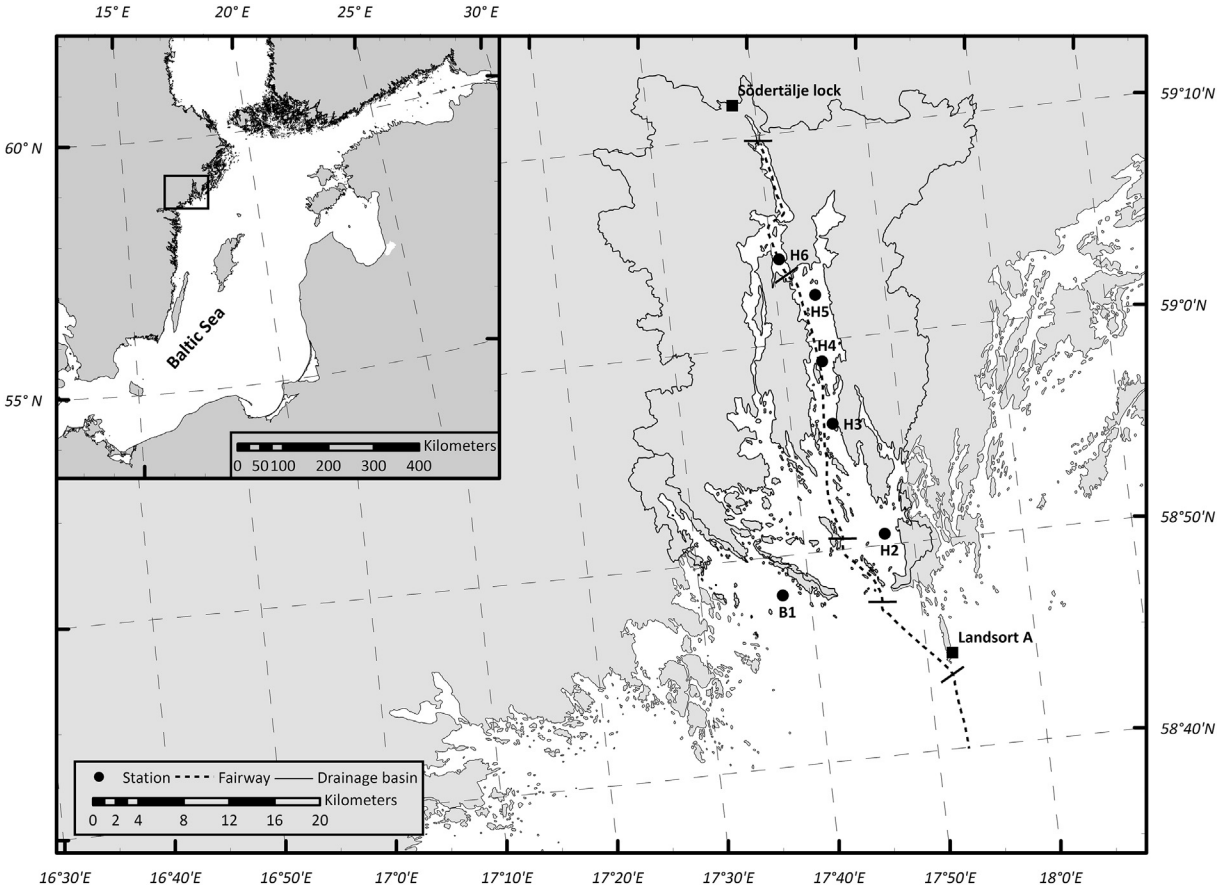

Fig. 1. Map of Himmerfjärden in the north-western Baltic proper with the sampling stations: H6 - H2 inside the bay and B1 offshore. The black line confines the drainage basin of Himmerfjärden. The squares show the weather station Landsort A (SMHI) and the Södertälje lock. The dashed line shows the fairways that were used to describe the ice conditions as the Baltic Sea Ice Code (SMHI), the fairways were divided from north to south as follows: Södertälje-Skanssundet-Fifång-Västra Röko-Landsort.

the ice cover, except for a few cases during the winters with a long ice season, when the Secchi depth was measured through a hole drilled into the ice.

The onset of the spring bloom was defined as the day of the year when Chl-a concentration had an increase rate of $\geq 0.2\,\mu g\,l^{-1}$ per 5 days *and* Chl-a concentration was $\geq 3.0\,\mu g\,l^{-1}$. The calculations were based on daily Chl-a values obtained from linearly interpolated in situ Chl-a measurements over each study period (from 1 January to 31 May). The spring bloom growth period was defined as the number of days from the timing of the spring bloom onset until the timing of the Chl-a maximum. Phytoplankton data are available at stations H4 and B1 for the whole study period 1997–2015 (see map, Fig. 1). Water samples (200 ml) were taken from the same vertically integrated hose samples as for deriving the chlorophyll concentration and preserved with 1 ml acetic Lugol's iodine solution. Phytoplankton biomass and abundance were determined using an inverted microscope according to HELCOM guidelines. In order to obtain biomass ($\mu g\,C\,l^{-1}$), cell numbers were multiplied by species- and size-class-specific volumes and carbon contents (Olenina et al., 2006). In this study, the phytoplankton composition and biomass is reported on a group level; e.g. diatoms, dinoflagellates. As the ciliate *M. rubrum* is rather common in spring, it is reported on the species level. The proportion of dinoflagellates was calculated as the biomass of dinoflagellates divided by the combined biomass of diatoms, dinoflagellates and *M. rubrum*.

In addition to the monitoring dataset, bio-optical in situ campaigns were performed in 2010 (5, 18 and 24 May), 2012 (27 April, 3, 10 and 21 May), 2014 (11 February, 10 March, 1 and 29 April), and 2015 (10 February, 11 March, 22 April and 21 May) in order to retrieve information on turbidity, the concentration of SPM as well as CDOM absorption, and thus, water quality. Water samples were collected from just below the sea surface to avoid floating matter. The CDOM samples were filtered through a membrane filter (0.2 µm) with a mild, 200 mbar vacuum within 24 h (Kratzer, 2000; Harvey et al., 2015). Filtered CDOM samples were stored in a fridge (+4 °C) for up to 3 months. CDOM absorption was measured spectrophotometrically against ultrapure water in a 100 mm cuvette, using a Shimadzu UVPC 2401 dual-beam spectrophotometer. The absorbance spectrum was corrected for the average absorbance between 700 and 750 nm according to D'Sa et al. (1999) to account for measurement errors. The absorption coefficient at 440 nm (g_{440}) was derived to indicate the CDOM absorption (Kirk, 2011). As CDOM is mostly of terrestrial origin and is carried into the sea by freshwater, it is inversely related to salinity, but this is mainly documented for summer data (Højerslev et al., 1996; Kratzer et al., 2003, 2011; Kowalczuk et al., 2006; Harvey et al., 2015). Here, a local relationship for spring was derived for CDOM absorption against surface salinity based on the available measurements from February to May. Concentration of SPM was measured gravimetrically according to Strickland and Parsons (1972) and turbidity in FNU (Formazin Nephelometric Unit) according to ISO 7027 method. These methods are described in detail in Kari et al. (2016).

In order to examine the spatial gradients as well as the effects of the under-ice plume onto the studied parameters, we performed a linear mixed effects model for each parameter with an interaction between under-ice plume (a yes/no indicator) and station (factor with five levels) set as fixed effects on the models, and year as a random factor. Linear mixed effects models evaluate the effects of the fixed variables

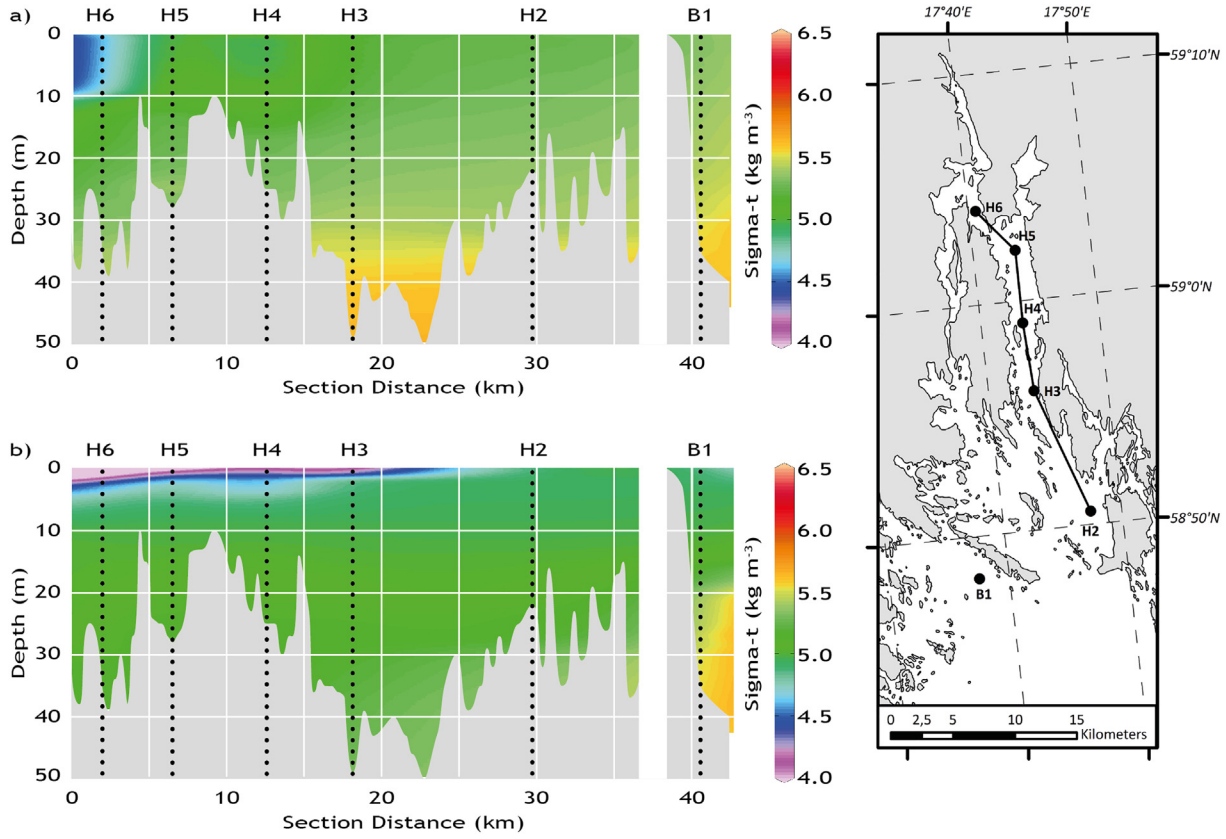

Fig. 2. Density stratification (Sigma-t) along a transect from the head of the bay (Station H6) to the open sea (Station B1) during spring a) without an under-ice plume, where fresh water is mixed at H6 and density gradually increased towards the open sea (March 2012) and b) with a distinct under-ice plume. The river plume is about 5 m thick and reaches beyond the station H4 (March 2010). The bottom topography was estimated based on a navigational map.

while accounting for the effect of the random variables (Quinn and Keough, 2002; Zuur et al., 2009). Statistical analyses were performed using R v. 3.0.1 (R Core Team, 2017). We performed linear mixed effects models with the lme-function from the nlme-package (Pinheiro et al., 2017). The statistical significance of the models was obtained by likelihood ratio tests i.e. comparing model to model without any fixed effects. All model results were tested with a Wald's significance test using the Anova-function from the car-package (Fox and Weisberg, 2011). Significance level was set to $\alpha = 0.05$. When a significant interaction between stations was found, the interaction was assessed through Tukey's all-pair comparison with the lsmeans-function in the lsmeans-package (Lenth, 2016).

3. Results

Stratification development within Himmerfjärden was examined along a transect from the head of the bay (H6) out to the offshore station (B1) (Fig. 2). In a typical case (n = 14), no under-ice plume occurred and runoff affected the water density mostly at station H6, and was mixed deeper into the water column (Fig. 2a). Distinct under-ice plumes were found during five years (Table 1), reaching stations H6 to H4. In two cases, the under-ice plume reached even the station H3 in the middle of the bay (Fig. 2b). Over the study period, the average temperature of the upper layer (0–5 m) for March was significantly different between stations, decreasing from the head of the bay to the open sea ($p < 0.001$). In years with an under-ice plume, the water temperatures were lower at all measurement stations (Table 2). The mean temperature of all stations during an under-ice plume ranged from −0.2 °C to 1.6 °C, while without the under-ice plume it ranged from 0.4 °C to 3.0 °C. During our study period, from January to April, the density stratification in Himmerfjärden was salinity-driven. The average salinity of the upper layer (0–5 m) in March differed significantly between the stations ($p < 0.001$), increasing from the head of the bay to offshore. Average salinity of the upper 5 m was lower during an under-ice plume only at B1 (data not shown), but the surface salinity (0–1.5 m), was significantly lower at all stations (Table 2). During an under-ice plume, surface salinity across all stations ranged from 4.9 ppt to 6.5 ppt, while without a plume the range was 4.7 ppt to 7.1 ppt. Both surface temperature and surface salinity were significantly lower during the years with an under-ice plume at all stations, even at the offshore station B1. Nevertheless, the distinctive under-ice plume did not reach the offshore station, as the plume water was mixed within the water column closer to the head of the bay. The differences in surface temperature and salinity at B1 were caused by generally lower temperatures during spring and the lack of mixing due to ice cover and freshwater input from thawing ice. All in all, an under-ice plume occurring in Himmerfjärden showed no direct effects at B1.

In years with under-ice plumes, the ice seasons were clearly longer as indicated by the Baltic Sea ice codes (Table 2). In these years (n = 5, 26% of studied years), the ice cover extended across all stations. Due to the extensive ice cover, the wind-driven mixing was limited and the water column stabilized, allowing for the under-ice stratification to develop. The shortest ice season leading to an under-ice plume was 98 days at head of the bay (H6), 86 days at middle of the bay (H5-H3), and 21 days offshore (fairway from Västra Röko to Landsort) (Table 1). For example, in 1996/97 no under-ice plume occurred in March, although the ice season length was 76 days at station H6, and 75 days at H5-H3, and 20 days offshore (fairway from Västra Röko to Landsort). The ice season length leading to an under-ice plume was on average 109 days at H6 and 101 days at H5-H3 (Table 1), these are 5.5 and 5.1 times the surface water (0–10 m) retention time (20 days) in Himmerfjärden. Here, we focus on the stratification patterns during March

Table 1
Annual information about the occurrence of under-ice plume events (* indicates a year with an under-ice plume), mean daily temperature (°C), cumulative precipitation (mm), and runoff from 1st January to 30th April each year. The ice season length in days is based on Baltic Sea ice codes from the head of the bay (H6) to offshore (Västra Röko-Landsort).

Year (Spring)	Mean daily temperature (°C)	Cumulative precipitation (mm)	Cumulative runoff (mm)	Sea ice season length (days)			Ice break-up (day of the year)			Spring bloom onset (day of the year)			Date of Chl-a maximum (day of the year)		
				H6	H5-H3	offshore	H6	H5-H3	offshore	H6	H4	B1	H6	H4	B1
1997	1.0	69.4	180.6	76	75	20	70	70	28	62	74	80	93	105	91
1998	1.3	120.5	190.1	0	0	0	–	–	–	68	78	92	106	98	96
1999	1.1	155.2	214.5	47	12	NA	55	55	–	92	91	91	112	98	96
2000	1.8	76.4	167.6	49	18	NA	73	43	–	38	82	91	90	97	96
2001	0.7	98.4	257.8	38	0	0	73	–	–	79	77	82	108	99	92
2002	2.2	87	378.0	40	40	NA	51	51	–	92	93	86	106	106	92
2003*	**−0.3**	**67**	**207.0**	**100**	**86**	**53**	**90**	**90**	**82**	**86**	**81**	**74**	**98**	**91**	**84**
2004	0.9	82.7	200.6	58	38	13	60	60	78	81	82	86	96	96	92
2005	0.9	72.5	184.1	68	55	6	96	93	70	43	47	64	88	76	88
2006*	**−0.8**	**86.8**	**214.3**	**105**	**101**	**59**	**111**	**107**	**95**	**96**	**89**	**89**	**115**	**108**	**94**
2007	2.2	117	170.7	35	31	2	73	69	42	89	93	89	114	114	92
2008	3.3	114	170.8	0	0	0	–	–	–	74	74	65	99	106	86
2009	1.2	69.5	203.2	49	45	3	75	75	10	75	79	87	127	118	96
2010*	**−1.5**	**85.5**	**219.3**	**98**	**98**	**61**	**102**	**102**	**91**	**99**	**84**	**86**	**124**	**109**	**96**
2011*	**0.4**	**57.3**	**206.9**	**132**	**121**	**57**	**99**	**93**	**75**	**93**	**85**	**88**	**108**	**108**	**94**
2012	1.4	94.4	197.8	60	50	1	89	81	36	75	77	88	108	108	93
2013*	**−0.3**	**57.6**	**223.4**	**112**	**101**	**21**	**119**	**119**	**82**	**66**	**87**	**87**	**106**	**113**	**99**
2014	2.6	122.7	217.7	5	5	0	34	34	–	75	80	93	105	105	98
2015	3.2	129.9	180.6	0	0	0	–	–	–	37	75	80	112	98	98

around the spring bloom onset. Shorter ice seasons could have led to smaller-scale, temporary under-ice plumes earlier in the ice season. However, the five defined years with under-ice plumes were established and distinctive during March and remained discernible up to about 1 month after the ice break up, i.e. until the end of April.

According to FMI's ice charts, the ice seasons from 1996/97 to 2014/15 in the Baltic Sea varied from extremely mild to severe. The maximum ice cover area in the Baltic Sea varied from only 49,000 km^2 (2007/08) to 309,000 km^2 (2010/11). Seven mild ice seasons (sea ice cover area < 115,000 km^2) occurred during the studied time period, two of them were extremely mild with ice cover area 49,000 km^2 (2007/08) and 51,000 km^2 (2014/2015), respectively. According to the Baltic Sea ice codes, the ice season length at the head of Himmerfjärden bay ranged from 0 days (1997/98, 2007/08, and 2014/15) to 132 days (2010/11) and the sea ice extent from no ice cover to covering all monitoring stations (Table 1). During the years when sea ice occurred, the ice break-up, i.e. the last day of ice cover, was earliest at the beginning of February (day 34 of the year) and latest at end of April (day 119) in the inner Himmerfjärden (H6-H5), while offshore (Västra Röko - Landsort) the ice break-up was earliest in mid-January (day 10) and latest in early April (day 95). The yearly mean of daily air temperatures (for 1st January to 30th April) 1997–2015 ranged from −1.5 °C in 2010 to 3.3 °C in 2008 with a median of 1 °C (Table 1). During the same time period, the cumulative precipitation (sum of daily precipitation over the same period) varied from 57 mm (in 2011) to 155 mm (1999) with a median of 87 mm. Wind data was averaged for the spring period from 1st February until 30th April. January was excluded from the analysis as to avoid biases caused by winter storm events, which are typical from December to January in the study area. The prevailing wind direction during spring in 1997–2015 was southwest. The cumulative runoff (from 1st January to 30th April) varied from 168 mm (2000) to 378 mm (2002) with a median of 203 mm (2009). Neither the cumulative runoff nor the cumulative modeled global irradiance data (SMHI) showed any significant differences over the years ($p > 0.4$ and $p > 0.9$, respectively) nor any differences between the years with or without under-ice plumes ($p > 0.2$ and $p > 0.5$).

A steady increase in Secchi depth was observed from the head of the bay towards the open sea ($p < 0.001$). During an under-ice plume, measured Secchi depth at station H3 was on average 6.2 m while without an under-ice plume the average was 5.0 m (Table 2). The Secchi depth was also deeper at stations H6 and H4 during an under-ice plume, while at stations H5 or B1 there were no significant effects of under-ice plume (Table 2). The CDOM dataset was collected in the spring of 2010, 2012, 2014, and 2015. The measured CDOM absorption at 440 nm (g_{440}) ranged from 0.33 to 1.10 m^{-1}, with a median of 0.53 m^{-1}. There was a clear spatial gradient of decreasing CDOM absorption from the head of the bay to the open sea. Mean g_{440} was 0.86 m^{-1} at H6 (n = 8), 0.66 m^{-1} at H4 (n = 11), 0.57 m^{-1} at H3 (n = 9), 0.46 m^{-1} at H2 (n = 10), and 0.42 m^{-1} at the offshore station B1 (n = 13). CDOM and surface (0–1.5 m) salinity showed a strong correlation with a correlation coefficient $r = 0.68$ (n = 53). The following linear regression was used to estimate CDOM based on surface salinity:

$$g_{440} = -0.276 \bullet S + 2.24 \quad (1)$$

where g_{440} stands for the CDOM absorption at 440 nm (unit: m^{-1}) and S for surface salinity (unit: ppt) (Fig. 3). For the intercept and the slope, the standard deviation was 0.25 and 0.04, respectively. The residual standard error was 0.13 m^{-1} (df = 51). Since the points in the g_{440}-salinity diagram are almost on a straight line, CDOM absorption and salinity can be interpreted here as mixing of two water types, runoff water and Gotland Basin water. The former is freshwater with high CDOM absorption while the latter is brackish water with low CDOM absorption from the open sea. However, g_{440} does not approach zero, but levels out to a rather low value, and declines again in the open sea with increasing salinity. Taking the representative salinity as 7 ppt for the northern Gotland Basin, the predicted g_{440} would be 0.31 m^{-1}. According to in situ data by Kratzer and Tett (2009), salinity in summer was on average about 5.7 in the top layer and the g_{440} values ranged from 0.33 m^{-1} to 0.39 m^{-1} (n = 3) at the Landsort Deep (BY 31, 58.583°N 18.233°E). Since the freshwater inflow was kept near the bottom of the ice in the event of an under-ice plume, the predicted g_{440}-values were higher at all stations than during the years without ice cover or with only short ice season. The estimates for g_{440} ranged from 0.44 m^{-1} to 0.90 m^{-1} during years with an under-ice plume, whereas years without plumes showed a somewhat larger range in g_{440}, i.e. from

Table 2
Results for the studied parameters. Left: mean values of each parameter with and without an under-ice plume over the study period 1997–2015. Temperature, surface salinity, Secchi depth, CDOM absorption (g_{440}) and mean Chl-a concentration were averaged over March each year. Right: Results of linear mixed effects models assessing the differences between years with and without under-ice plume for each parameter. Differences were assessed through Tukey's all-pair comparison of means. Significant differences are indicated in bold.

Parameter	Mean (1997–2015)		Under-ice plume - No under-ice plume		
	Plume	No plume	Difference	Standard error	p-value
Temperature (0–5 m depth) (°C)					
H6 (head of bay)	0.8	1.6	**−0.8**	0.35	**0.034**
H4 (mid-bay)	0.5	1.3	**−0.8**	0.36	**0.030**
B1 (offshore)	0.1	1.4	**−1.3**	0.35	**0.002**
Surface salinity (0–1.5 m depth) (ppt)					
H6 (head of bay)	5.3	5.5	**−0.4**	0.14	**0.006**
H4 (mid-bay)	5.8	6.0	**−0.5**	0.14	**0.004**
B1 (offshore)	6.3	6.6	**−0.3**	0.14	**0.035**
Ice season length (no. days with ice cover)					
Head of bay	109	38	**72**	10.96	**< 0.0001**
Mid-bay	101	26	**75**	10.96	**< 0.0001**
Offshore	50	4	**46**	11.09	**< 0.001**
Secchi depth (m)					
H6 (head of bay)	4.8	3.6	1.2	0.60	0.066
H3 (mid-bay)	6.2	5.0	**1.3**	0.60	**0.049**
B1 (offshore)	8.5	8.2	0.3	0.60	0.591
CDOM absorption (g_{440}) estimate (m^{-1})					
H6 (head of bay)	0.87	0.76	**0.12**	0.04	**0.006**
H4 (mid-bay)	0.71	0.58	**0.13**	0.04	**0.004**
B1 (offshore)	0.51	0.42	**0.09**	0.04	**0.035**
The onset of phytoplankton spring bloom					
H6 (head of bay)	88	70	**18**	7.26	**0.024**
H5 (inner bay)	89	74	15	7.26	0.054
B1 (offshore)	85	84	1	7.26	0.898
Mean Chl-a concentration in March ($\mu g\,C\,l^{-1}$)					
H6 (head of bay)	1.9	4.6	**−2.7**	1.01	**0.015**
H4 (mid-bay)	2.0	3.6	−1.6	1.01	0.134
B1 (offshore)	1.9	1.9	0.0	1.01	0.997
Maximum Chl-a concentration ($\mu g\,C\,l^{-1}$)					
H6 (head of bay)	15.5	14.9	0.6	2.49	0.814
H4 (mid-bay)	16.7	15.8	3.1	2.49	0.223
B1 (offshore)	7.0	5.6	1.3	2.49	0.595
The timing of the maximum Chl-a concentration					
H6 (head of bay)	110	105	6	4.25	0.203
H4 (mid-bay)	106	102	5	4.25	0.253
B1 (offshore)	93	93	0	4.25	0.978

$0.28\,m^{-1}$ to $0.95\,m^{-1}$.

During the measurement campaigns in 2014 and 2015, turbidity ranged from 0.5 FNU to 4.9 FNU (median 1.4 FNU). The maximum turbidity was measured at the head of the bay (H6) in February 2014. The head of the bay remained turbid in March 2014 with 3.4 FNU, while in May 2015 the highest measured turbidity was 2.5 FNU. Turbidity decreased towards the open sea during both years. At station B1, turbidity ranged from only 0.5 FNU to 1.0 FNU. As a measure of particle scatter, turbidity depends on the SPM in the water column, and thus is likely to be affected by shore erosion and resuspension of bottom sediments. The SPM concentrations at all stations ranged from $0.4\,g\,m^{-3}$ to $4.5\,g\,m^{-3}$ (median $1.3\,g\,m^{-3}$). At every sampling occasion, there was a spatial gradient of decreasing SPM from the head of the bay towards the open sea. The average SPM concentration was $2.6\,g\,m^{-3}$ at H6 and $0.7\,g\,m^{-3}$ at B1. During February 2014 it was highest at station H6 and decreased from $4.5\,g\,m^{-3}$ to $2.3\,g\,m^{-3}$ by late April. During February 2015, SPM was only $1.4\,g\,m^{-3}$ and increased to $3.4\,g\,m^{-3}$ by late May. These ranges and distribution patterns of SPM concentrations and turbidity are typical for the study site (Kratzer and Tett, 2009; Kari et al., 2016). The inorganic SPM in this study decreased both geographically towards the open sea and seasonally from February to May. The proportion of inorganic SPM from the total concentration of SPM ranged from 82% inside the bay (H3) to 27% offshore (B1), with a median of 54.1%.

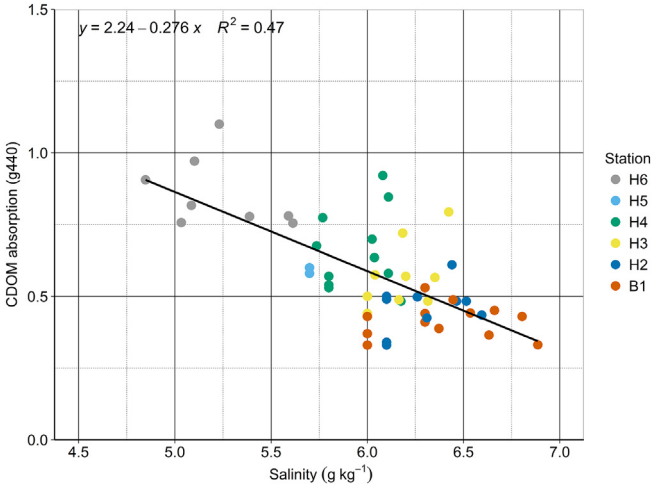

Fig. 3. Regression between CDOM absorption (g_{440}) and salinity (ppt). The colors represent the different monitoring stations along the Himmerfjärden bay, from the head of the bay (H6) to the offshore station (B1).

Fig. 4 illustrates the timing of the phytoplankton spring bloom onset (day of the year) and its spatial gradient along the monitoring stations. During years with an under-ice plume, the onset tends to be earliest close to the middle of the bay (H3), and subsequently spreads further both to the head of the bay (H6) and further offshore (B1). In springs without any under-ice plume, the spring bloom starts earlier at the head of the bay (H6) progresses towards the mouth of the bay (H3) and appears slightly later at the offshore station (B1). This interactive effect of the under-ice plume and station was statistically significant ($p < 0.01$). When the under-ice plume occurred, the onset of the spring bloom was delayed by about 18 days at H6, while the effect was not significant at other stations (Table 2). Due to the under-ice plume characteristics, the surface salinity decreased during these events. The indirect effect of surface salinity on the timing of the spring bloom onset was analyzed and found to be significant. There was a significant interactive effect of surface salinity and station ($p = 0.03$). At station H6, decreased salinity was associated with a delay of bloom onset by 22 days on average ($p < 0.01$). This was not observed at any other station. During an under-ice plume, there was an interactive effect between bloom onset and ice break-up ($p < 0.001$): the bloom onset at H6 was delayed on average by 0.8 days per additional day with ice cover ($p = 0.04$), whereas at H3 the bloom onset was advanced by 1 day per additional day with ice cover ($p = 0.02$).

The under-ice plume had a significant effect on the average Chl-a concentration in March only at station H6; during years with an under-ice plume, the Chl-a concentration was on average $2.7\,\mu g\,l^{-1}$ lower than in years without an under-ice plume (Table 2). In contrast to the timing of the spring bloom onset, neither the maximum concentration

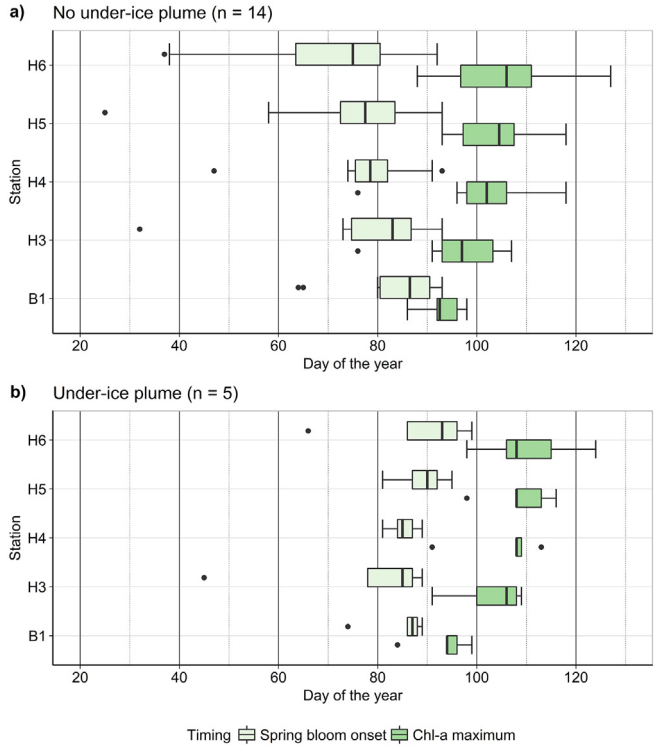

Fig. 4. Timing of the spring bloom onset (light green) and the timing of the Chl-a maximum (dark green) during a) years without an under-ice stratification and b) years with an under-ice plume. In the boxplot, the midline shows the median, the upper and lower limits of the box show the third and first quartile, respectively. The whiskers extend up to 1.5 times the interquartile range and the dots represent outliers. (For interpretation of the references to colour in this figure legend, the reader is referred to the web version of this article.)

of Chl-a, nor the timing of the Chl-a maximum were significantly affected by the under-ice plume (Table 2). The Chl-a concentration reached maxima (Fig. 4) in mid-April at stations H6 and H4 (days 106 and 103 of the year, respectively) and early April at station B1 (93). At station H6, the spring bloom growth period, defined as the number of days from the bloom onset until the timing of the Chl-a maximum, was about 12 days shorter when an under-ice plume occurred, while other stations showed no significant differences (Table 2). A shorter growth period indicates a higher daily productivity at station H6 during an under-ice plume.

The phytoplankton community was analyzed at stations H4 and B1. Table 3 shows the biomass of the main phytoplankton groups: dinoflagellates, diatoms, and the ciliate *M. rubrum*, during the spring bloom growth period (from onset to maximum) with and without the occurrence of an under-ice plume. Dinoflagellate biomass showed no significant differences, neither with regards to the under-ice plume nor between the stations ($p > 0.2$). At station H4, the diatom biomass was on average 84 µg C l^{-1} higher and *M. rubrum* 39 µg C l^{-1} lower in years with an under-ice plume (Table 3), but at B1 biomasses were not significantly affected (Table 3). Since there was no difference in dinoflagellate nor in total phytoplankton biomass, the dinoflagellate proportion was not affected by the plume (Table 3).

In addition to the plume/no plume classification, the dataset was divided into three classes by the ice season length at the head of the bay: years with the number of ice days < 7 (n = 4), years with ice cover but no under-ice plume (n = 10), and years with a plume (n = 5). The only phytoplankton group that showed a significant difference between these classes was the biomass of *M. rubrum* at station H4 during the growth period ($p < 0.01$). During the years with an under-ice plume the *M. rubrum* biomass was on average 19 µg C l^{-1}, while it was 38 µg C l^{-1} in the years with some ice cover but no distinct under-ice plume and 109 µg C l^{-1} in the years with < 7 days of ice cover. Thus, *M. rubrum* seems to favor ice-free and turbulent conditions during mild winters.

4. Discussion

During the study period (1997–2015) ice seasons varied from extremely mild to severe in the Baltic Sea. Since the beginning of observations in 1720, the two mildest ice seasons occurred in 2007/08 and 2014/2015 (Seinä and Palosuo, 1996; Uotila et al., 2015). In these years, Himmerfjärden was ice-free, except for a short period in the innermost bay. The length of the ice season varied greatly in Himmerfjärden with ice break-up dates from the beginning of February to the end of April. Our results confirmed that the development of the under-ice stratification is a common phenomenon in Himmerfjärden, given the ice season is long enough to stabilize the water column. During the study period, distinctive under-ice plumes occurred in 5 out of 19 spring seasons. An under-ice plume developed only during cold winters with a mean daily temperature < 0.4 °C and when all stations were ice-covered for a sufficient amount of time. The shortest ice season leading to an under-ice plume was 98 days at the head of the bay (H6) and 86 days at mid-bay (H5-H3), these are 5.5 and 5.1 times the retention time of the surface water (0–10 m) in Himmerfjärden. According to our results, shorter ice seasons and fewer years with complete ice-cover across the bay would lead to fewer under-ice plume events, and thus to

Table 3
Results from phytoplankton biomass per group. Left: Proportion of dinoflagellates and the biomass of the three main groups without and during under-ice plume in µg C l^{-1} at stations H4 and B1 during the growth period (from onset to maximum date). These are mean values of all measurements and their standard deviations for each spring during the study years 1999–2015. Right: Results of linear mixed effects models for each parameter evaluating the differences between years with and without an under-ice plume. Coefficients were assessed through Tukey's all-pair comparison of means. Significant differences are indicated in bold.

	Biomass during the growth period (µg C l^{-1})		Results of linear mixed effect models		
	No under-ice plume (n = 14)	Under-ice plume (n = 5)	Under-ice plume - No under-ice plume		
	mean ± st. dev.	mean ± st. dev.	Difference	Standard error	p-value
H4					
Dinoflagellates	19.4 ± 21.9	22.4 ± 26.2	3	14.01	0.833
Diatoms	138.0 ± 79.9	222.2 ± 111.7	**84**	36.09	**0.033**
Mesodinium	58.0 ± 51.1	18.7 ± 12.3	**−39**	17.36	**0.039**
Proportion of dinoflagellates	8% ± 0.07	9% ± 0.08	1%	6.37	0.918
B1					
Dinoflagellates	29.1 ± 31.5	28.9 ± 27.6	0	14.15	0.998
Diatoms	64.9 ± 42.1	75.4 ± 24.6	7	36.43	0.847
Mesodinium	16.1 ± 8.0	10.2 ± 8.1	−6	19.05	0.768
Proportion of dinoflagellates	26% ± 0.17	19% ± 0.14	−7%	6.98	0.329

a change in phytoplankton composition.

During an under-ice plume, both the average water temperature of the top layer (5 m) and the surface (1.5 m) salinity were lower at all stations than during the years without a well-established under-ice plume. The under-ice plume was usually about 2 m thick in Himmerfjärden. In a study by Granskog et al. (2005), the plume thickness was also estimated to be about 1–2 m. Merkouriadi and Leppäranta (2015) showed four examples of under-ice plumes in the Gulf of Finland, and in all these cases, the under-ice plume was < 5 m thick. Thus, under-ice plumes offer a rather shallow and distinct environment for the spring bloom development. The sea ice cover allows for the stratification to develop and the thawing ice (and snow cover) provides the surface layer with additional freshwater input, which further stabilizes the stratification. The stratification becomes stable enough to affect the hydrographic conditions of the water column much longer after the ice has been broken up. In our study, the under-ice plume remained distinguishable even until the end of April, from one week to three weeks or even longer after the ice break-up. The under-ice plume was then broken up due to wind-driven mixing and thermal convection. The under-ice plume modifies the environmental conditions for phytoplankton in Himmerfjärden by transporting colder and less saline runoff further along the bay towards the open sea. Spring stratification in the Baltic Sea is driven by both freshwater advection and thermal convection (Eilola and Stigebrandt, 1998; Klais et al., 2011; Leppäranta and Myrberg, 2009; Stipa, 2002). Hence, in addition to the temporary effect of sea ice cover on the spring bloom onset, the under-ice plume affected the physical environment during the growth period of the spring bloom.

As CDOM is transported into the sea by runoff (Højerslev et al., 1996; Kratzer et al., 2003, 2011; Kowalczuk et al., 2006), it is inversely related to salinity. Thus, both CDOM and salinity can be used as markers for different water types: coastal runoff and Gotland Basin water. The results showed also strong correlation between air temperature and CDOM ($r = 0.62$, $p = 0.0046$). This can be explained by an increased input of CDOM-rich terrestrial meltwater. As the freshwater carries high loads of CDOM into coastal waters, under-ice plumes are expected to be rich in CDOM. The high CDOM absorption in turn, may be expected to reduce water transparency. In this study, CDOM was only measured during ice-free conditions. Thus, CDOM (g_{440}) was estimated with an empirical relationship from surface salinity (using Eq. (1)). Surface salinity decreased at all stations during an under-ice plume and correspondingly, the estimated CDOM absorption increased. Despite the higher CDOM absorption within the surface layer during an under-ice plume (Table 2), the Secchi depth was 1.3 m deeper at station H3 compared to those spring seasons without an under-ice plume. For the other stations, no significant difference in Secchi depth could be detected. In most cases (77 of 94 in total), the mixed layer was greater than the Secchi depth, both averaged over March each year, while most of the cases (14 of 17) when Secchi depth was greater than the mixed layer depth occurred during an under-ice plume.

In the Baltic Sea coastal waters, the water transparency is mostly governed by CDOM and SPM (Kratzer and Tett, 2009; Kratzer and Moore, 2018). Kratzer and Tett (2009) found that the concentration of SPM governs the variability of light attenuation in Himmerfjärden, despite the optical dominance of CDOM. CDOM shows a logarithmic decrease inside the bay from station H5 to H3 and then stays rather constant from station H2 until about 20 km off-shore (Kratzer and Tett, 2009). SPM, especially its inorganic fraction, shows a steep decline within Himmerfjärden, following the depth profile (Fig. 2) suggesting reduced resuspension and thus increasing net particle settling. This was also demonstrated in the bio-optical transects by Kratzer and Tett (2009) for summer, and the same pattern was shown in our bio-optical dataset for spring. The increased Secchi depth at station H3 during springs with an under-ice plume may thus be caused by the less turbulent conditions, the plume further enhancing the net settling of inorganic SPM, leading to less turbid, and thus more transparent surface waters. Unfortunately, there are no SPM measurements available during the ice seasons.

In the Baltic Sea, the phytoplankton community has an annual succession with a spring and a summer bloom during which the concentration of phytoplankton cells markedly exceeds the annual average concentration. Defining appropriate spring bloom metrics is not trivial as both intensity and onset of the spring bloom should be taken into account. Fleming and Kaitala (2006) defined a phytoplankton spring bloom intensity index taking into account both the Chl-a concentration and the duration of the bloom. Both are essential parameters when evaluating the influence of primary production on the food web. The authors defined a Chl-a concentration threshold of $5\,\mu g\,l^{-1}$, based on a dataset from 1992 to 2004 and any (daily) Chl-a concentrations higher than this threshold were included in the spring bloom intensity index. This index has been part of the HELCOM indicator reporting since 2003 as a tool to estimate phytoplankton dynamics in the Baltic Sea. However, this threshold was too high for a few stations in Himmerfjärden during some springs, and using this index would be misleading for our area of investigation. Alternatively, Groetsch et al. (2016) listed three groups of spring bloom metrics: based on a fixed threshold value of Chl-a concentration, a growth-rate and a distribution-rate metric. They used the following parameters: maximum, average and the sum of daily Chl-a concentrations during the spring bloom. In their study, daily Chl-a concentrations were available for such an analysis. For Himmerfjärden, however, there are only weekly measurements available from the local monitoring program during spring bloom periods, which were linearly interpolated to obtain daily values. Höglander et al. (2004) defined the spring bloom onset based on a 4-fold increase in Chl-a concentration from the pre-bloom level. In Himmerfjärden, the measurements are performed throughout the year, but only monthly during low phytoplankton biomass in winter. If comparing the Chl-a concentration to the previous measurement, the result will depend on measurement frequency. The higher the measurement frequency, the less likely it is for the Chl-a concentration to have increased 4 times since the previous measurement. On the other hand, during winter the measured Chl-a concentration can be very low and despite a 4-fold increase, the concentration prevails too low for an actual spring bloom onset. The onset of the spring bloom was therefore defined here based on both the increase rate (Chl-a $\geq 0.2\,\mu g\,l^{-1}$ per 5 days) and a pre-defined threshold (Chl-a $\geq 3.0\,\mu g\,l^{-1}$). The same threshold concentration was also used in a recent study by Kahru et al. (2016). Setting the same threshold for all stations allows for a comparison between stations. The spring bloom onset definition used in this study is thus optimized for the local, coastal Chl-a concentrations and is not affected by measurement frequency per se.

In Himmerfjärden, the mean timing of the phytoplankton spring bloom onset ranged from late January (day 25 of the year) to early April (day 99) with a median in late March (day 82). The mean timing of the onset corresponds well with previous studies. Beltrán-Abaunza et al. (2016) studied the spatial and temporal variability of phytoplankton in Himmerfjärden during 2002–2012, based on satellite data, Chl-a concentrations reached the threshold (Chl-a $\geq 3.0\,\mu g\,l^{-1}$) within the same time range. According to Klais et al. (2011), the typical timing for the spring bloom onset is late March (day 80) in our study region. Fleming and Kaitala (2006) found an average onset day in mid-April (day 101) during 1994–2004. During the corresponding years within this study, the average onset day was slightly earlier, i.e. at the beginning of April (day 94). Based on satellite data (1999–2013), Kahru et al. (2016) found that the timing of bloom onset was in early April (day 90). However, as discussed, the definition of bloom onset differs among studies. The cited studies were also performed in the open sea, whereas in our study, the stations are comparably coastal. The environmental conditions, such as ice conditions, stratification, and light conditions, differ clearly between open sea and coastal areas. The CDOM absorption and the scattering by SPM strongly affect the light conditions in the coastal areas, especially in the very inner bay, while in

the open sea the effect of SPM scattering is much less prevalent (Kratzer and Tett, 2009). Andersson et al. (2018) showed that CDOM affects phytoplankton growth rate negatively, while it favors bacterial production.

During the years with an under-ice plume, the onset of the phytoplankton spring bloom ranged over 33 days at H6, from early March (day 66 of the year) to early April (day 99) (Fig. 4). Without a distinct under-ice plume, the range was greater (55 days) from early February (day 37) to beginning of April (day 92). During an under-ice plume, the onset was delayed on average by 18 days at the head of the bay at H6. During under-ice plumes, decreased surface salinity was associated with a delay of spring bloom onset timing at H6. The under-ice plume may act as an additional light shield due to its higher CDOM absorption in the inner bay (H6-H4) as predicted from the developed CDOM-salinity model (Eq. (1)) and by the bio-optical model developed by Kratzer and Tett (2009). During the years with an under-ice plume, the ice break-up day affected the timing of bloom onset at station H6, the onset was delayed by 0.8 days per additional sea ice day in the spring. This is expected as sea ice, especially when snow-covered, dramatically reduces the solar irradiance entering the water column (e.g. Warren, 1982). However, at H3, the onset timing occurred 1 day earlier for every additional day of sea ice. Presumably this is caused both by the increased stability of the water column and by the improved illumination due to lower inorganic SPM load in the middle and the outer bay. Studying the direct effect of sea ice on the onset of the phytoplankton spring bloom is problematic due to the different nature (scale as well as coverage of our data sources). SMHI's Baltic Sea ice code data are based on ice conditions along the fairway sections, not single point measurements as the Chl-a concentration (see Fig. 1).

The under-ice plume affected also the timing of bloom onset spatially. During an under-ice plume, the spring bloom started at the middle of the bay and progressed both up north towards the head of the bay and down south towards the open sea. When no under-ice plume occurred, the spring bloom development started earlier at the head of the bay and progressed further towards the open sea. In the absence of an under-ice plume, freshwater from the river runoff is mixed deeper into the water column close to the head of the bay (H6), which seems to contribute to an earlier start of the bloom at the innermost stations compared to the outer stations. The development of stratification of the water column and the mixing events have an important role in supplying nutrients to the phytoplankton bloom. The under-ice plume transports nutrients further from the coastal areas to open sea potentially influencing the spatial patterns of the phytoplankton spring bloom. This may affect nutrient retention at the coastal sites, as phytoplankton are transported further offshore instead of sedimenting at the coastal sites.

The maximum Chl-a concentration was found on average in mid-April (day 101 of the year), ranging from mid-March (day 76) to early May (day 127). Neither the maximum Chl-a concentration, nor the timing of the Chl-a maximum were significantly affected by the under-ice plume. Other factors, such as nutrient and light availability, seem to determine the maximum Chl-a concentration. Generally, the main driver of bloom intensity is considered to be the availability of nutrients after the winter (Kahru and Nõmmann, 1990; Fleming and Kaitala, 2006; Groetsch et al., 2016). The respective growth-limiting nutrient varies regionally in the Baltic Sea. In the north-western Baltic proper, the spring bloom growth is typically nitrogen-limited (Snoeijs-Leijonmalm et al., 2017), but a large local loading of nitrogen may lead to phosphorus limitation in some coastal waters. Usually, in the Baltic proper, nitrogen is used up during the spring bloom, whereas the phosphorus levels are still high at the beginning of the summer (Walve and Larsson, 2010). In the open Baltic Sea, silica is normally sufficient for diatoms during the bloom, but in coastal areas a high nitrogen load may induce large diatom blooms and thus lower silica to limiting levels. However, Kremp et al. (2008) performed a mesocosm study in three consecutive springs to investigate the phytoplankton spring bloom and they concluded that variations of initial availability dissolved inorganic silica relative to availability of nitrate and phosphorus did not affect the phytoplankton composition.

As the bloom onset was delayed at H6 during the under-ice plume but the timing of the Chl-a maximum was not affected, the spring bloom growth period (from onset to maximum) was shorter compared to years with no under-ice plume. As soon as the spring bloom appeared, Chl-a concentration reached typical ranges at typical times. Hence, the under-ice plume seems to only have a temporary effect on Chl-a concentrations. Both the Chl-a concentration and the phytoplankton composition were vertically integrated samples (0–14 m in Himmerfjärden and 0–20 m at B1). Unfortunately, there is no data available on the vertical distribution of different phytoplankton groups or species. Thus, it is not possible to judge whether the under-ice plume influences the phytoplankton within or below the under-ice plume or if they are sinking within the water column. Despite this limitation, the available Chl-a and phytoplankton data indicate the differences between years with and without the under-ice plume. Both the spatial and temporal variability of Chl-a concentration were also observed in the medium-resolution imaging spectrometer (MERIS) images, where positive Chl-a anomalies (i.e. with higher Chl-a concentration than the long-term median) were found during spring months in 2006 and 2010, both years with under-ice plumes (Beltrán-Abaunza et al., 2016).

Stratification and light conditions may modify not only the onset of the spring bloom but also its species composition. The phytoplankton composition is monitored at stations H4 (mid-bay) and B1 (offshore). During an under-ice plume, the diatom biomass increased markedly at station H4, while the biomass of *M. rubrum* decreased compared to years without an under-ice plume. Dinoflagellate biomass (or its proportion of the biomass of the main groups) was not significantly affected by the under-ice plume. The under-ice plume did not have significant effects on phytoplankton groups at B1. Unfortunately, no phytoplankton data are available from H6, which was mostly affected by the under-ice plume. However, the changes in phytoplankton composition and biomass that have been found at H4 are expected to be even more pronounced at H6, as the phytoplankton is transported south from station H6 along the surface currents. The most common phytoplankton groups in Baltic Sea ice are diatoms and dinoflagellates along with many other organisms, such as heterotrophic flagellates and ciliates including the mixotroph *M. rubrum* (Haecky et al., 1998; Kaartokallio, 2004; Piiparinen et al., 2010). Commonly, diatoms tend to settle out in low turbulent conditions (e.g. Margalef, 1978). However, ice cover provides a habitat for diatoms within the brine channels, which may establish a seed population for the spring bloom (Haecky et al., 1998; Piiparinen et al., 2010). Our study indicates that the seeding effect of ice can be more important for dominance of diatoms, or that they can remain in the upper shallow under-ice plume thus gaining from better light conditions. In addition, some diatom species can form filamentous colonies or have long thin spines protruding from the cells, increasing their buoyancy, and thus they can stay easier in suspension. After milder winters, when no under-ice plumes occur, diatoms were still the dominant phytoplankton group during the growth period (from onset to Chl-a maximum), but the ciliate *M. rubrum* had the second largest biomass (on average) rather than dinoflagellates. During years with < 7 days ice cover, *M. rubrum* biomass was markedly higher than during years with an under-ice plume. *M. rubrum* thus seems to favor ice-free, and thus more turbulent conditions during milder winters. In the coastal Baltic Sea and in Himmerfjärden, nutrients are abundant and do not limit the early growth of the spring bloom (unpublished monitoring data). This suggests that being motile is not an essential advantage for nutrient competition at the beginning of the spring bloom, but for other factors, such as better light conditions.

Taken together, the later onset timing favors the rapidly growing diatoms, while earlier onset favors *M. rubrum*. This shift in the species composition at the first part of the spring bloom can have consequences on the later part of the spring bloom.In Himmerfjärden, zooplankton

have their main growth period as late as in June–July (Rudstam et al., 1992). Therefore, the changes in the spring bloom are expected to have little direct effects on the population dynamics of zooplankton. However, if the under-ice plume changes nutrient transport and cycling in the coastal area, this may influence summer productivity. Phytoplankton composition and distribution has a high temporal and spatial variability and thus high-resolution observations are essential to further investigate the phytoplankton dynamics and their interactions with the physical conditions in the Baltic Sea (Lips et al., 2014; Beltrán-Abaunza et al., 2016). Under-ice plumes are not a typical case for Himmerfjärden, but as there has been a tendency towards shorter ice seasons, there is a strong case to assume that under-ice plumes have been more typical in the past. Therefore, this study can give an indication for what happens at other coastal sites that are, or will, undergo these environmental changes in the future, for example bays in the northern Baltic Sea.

5. Conclusions

Distinctive under-ice plumes were observed in 5 out of 19 springs during the study period (1997–2015). The under-ice plume modified the physical conditions in Himmerfjärden for the initiation and development of the phytoplankton spring bloom. Under-ice plumes formed during long ice seasons, when the ice covered the whole bay stabilising the stratification of the water column. Freshwater runoff, both from terrestrial and fluvial origin, created an about 2 m thick top layer, i.e. an under-ice plume. During springs with less or no ice cover, the freshwater was mixed directly at the head of the bay. Although CDOM absorption was higher within the under-ice plume, the Secchi depth increased during the springs with an under-ice plume. The under-ice plume stabilizes the stratification, which seems to reduce particle resuspension - and thus light attenuation – and therefore seems to improve the under-water light conditions for phytoplankton. The phytoplankton spring bloom onset was defined here based both on an increase rate (Chl-a $\geq 0.2\,\mu g\,l^{-1}$ per 5 days) and a threshold Chl-a concentration (Chl-a $\geq 3.0\,\mu g\,l^{-1}$). Optimizing the onset definition for the local, coastal sites allowed for a feasible comparison of onset timing between years. When the under-ice plume occurred, the spring bloom onset was delayed by about 18 days at station H6 ($p = 0.02$), while the effect was not significant at other stations ($p > 0.05$). However, the timing and magnitude of the maximum Chl-a concentration were not affected by the under-ice plume at any station. Thus, at H6 the growth period was on average 12 days shorter during an under-ice plume, indicating more intense growth once the biomass increase started. This shows that changes in climate can have different effects on the timing of the onset vs. the timing of the maximum of the spring bloom. These effects seem to depend on the location, presence of sea ice and the development of under-ice plumes. The phytoplankton composition at H4 was affected by the under-ice plume. During the growth period (from onset to Chl-a maximum), diatoms clearly dominate the phytoplankton community in both cases but had even higher biomass during a plume ($p = 0.03$). However, when no under-ice plume occurred, *M. rubrum* biomass was notably increased compared to years with a plume ($p = 0.04$). When the ice season was very short (< 7 days), the biomass of *M. rubrum* was markedly higher than in years with longer ice season. Thus, the more dynamic conditions in years without any under-ice plumes seem to favor the motile ciliate *M. rubrum*.

Acknowledgements

This study was funded by the Swedish National Space Board (project number SNSB Dnr. 147/12), by Nordforsk (project 42041) and by Baltic Ecosystem Adaptive Management (BEAM), – a Swedish strategic marine research project at Stockholm University (application number 2009-3435-13495-18) administered by the Swedish Research Council for Environment, Agricultural Sciences and Spatial Planning (Formas). Faculty funding was received from the Department of Ecology, Environment and Plant Science (DEEP) at Stockholm University as well as the Department of Physics at University of Helsinki, Finland. We also thank the monitoring group at DEEP for the valuable in situ data from the Himmerfjärden research and monitoring program (funded by SYVAB) as well as data from the national marine monitoring station B1 funded by the Swedish Environmental Protection Agency and the Swedish Agency for Marine and Water Management. The Baltic Sea Ice Code data were provided by the Ice Service from the Swedish Meteorological and Hydrological Institute (SMHI). STRÅNG data used here are from the SMHI and were produced with support from the Swedish Radiation Protection Authority and the Swedish Environmental Protection Agency. The Finnish Meteorological Institute (FMI) provided the ice charts and data for the maximum ice extent of the Baltic Sea. We also thank Elisa Alonso Aller (DEEP) for helping with the statistical analysis and Arttu Jutila at the Department of Physics (University of Helsinki) for creating the map of Himmerfjärden (Figs. 1 and 2) and Emilia Ellilä for the visualization of data in Fig. 2.

References

Andersson, A., Brugel, S., Paczkowska, J., Rowe, O.F., Figueroa, D., Kratzer, S., Legrand, C., 2018. Influence of allochthonous dissolved organic matter on pelagic basal production in a northerly estuary. Estuar. Coast. Shelf Sci. 204, 225–235.
Beltrán-Abaunza, J.M., Kratzer, S., Höglander, H., 2016. Using MERIS data to assess the spatial and temporal variability of phytoplankton in coastal areas. Int. J. Remote Sens. 1–25.
D'Sa, E.J., Steward, R.G., Vodacek, A., Blough, N.V., Phinney, D., 1999. Determining optical absorption of colored dissolved organic matter in seawater with a liquid capillary waveguide. Limnol. Oceanogr. 44, 1142–1148.
Eilola, K., Stigebrandt, A., 1998. Spreading of juvenile freshwater in the Baltic proper. J. Geophys. Res. Oceans 103, 27795–27807.
Engqvist, A., 1996. Long-term nutrient balances in the eutrophication of the Himmerfjärden estuary. Estuar. Coast. Shelf Sci. 42, 483–507.
Engqvist, A., Omstedt, A., 1992. Water exchange and density structure in a multi-basin estuary. Cont. Shelf Res. 12, 1003–1026.
Engqvist, A., Stenström, P., 2009. Flow regimes and long-term water exchange of the Himmerfjärden estuary. Estuar. Coast. Shelf Sci. 83, 159–174.
Fleming, V., Kaitala, S., 2006. Phytoplankton spring bloom intensity index for the Baltic Sea estimated for the years 1992 to 2004. Hydrobiologia 554, 57–65.
Fox, J., Weisberg, S., 2011. An R Companion to Applied Regression. Second. Sage Publications, Thousand Oaks (CA).
Granskog, M.A., Ehn, J., Niemelä, M., 2005. Characteristics and potential impacts of under-ice river plumes in the seasonally ice-covered Bothnian Bay (Baltic Sea). J. Mar. Syst. 53, 187–196.
Granskog, M.A., Kaartokallio, H., Kuosa, H., Thomas, D.N., Vainio, J., 2006. Sea ice in the Baltic Sea - a review. Estuar. Coast. Shelf Sci. 70, 145–160.
Groetsch, P.M.M., Simis, S.G.H., Eleveld, M.A., Peters, W.M., 2016. Spring blooms in the Baltic Sea have weakened but lengthened from 2000 to 2014. Biogeosci. Discuss. 13 (17), 4959–4973.
Haapala, J., Ronkainen, I., Schmelzer, N., Sztobryn, M., 2015. Recent change—Sea ice. In: BACC II Author Team (Ed.), Second Assessment of Climate Change for the Baltic Sea Basin. Springer International Publishing, pp. 1–501.
Haecky, P., Jonsson, S., Andersson, A., 1998. Influence of sea ice on the composition of the spring phytoplankton bloom in the northern Baltic Sea. Polar Biol. 20, 1–8.
Håkanson, L., Stenström-Khalili, M.I., 2010. How important are local nutrient emissions to eutrophication in coastal areas compared to fluxes from the outside sea? A case-study using data from the Himmerfjärden bay in the Baltic Proper. In: Friedman, A.G. (Ed.), Lagoons: Biology, Management and Environmental Impact. Nova Science Publisher, Inc., New York, United States, pp. 1–6.
Harvey, E.T., Kratzer, S., Andersson, A., 2015. Relationships between colored dissolved organic matter and dissolved organic carbon in different coastal gradients of the Baltic Sea. Ambio 44, 392–401.
Höglander, H., Larsson, U., Hajdu, S., 2004. Vertical distribution and settling of spring phytoplankton in the offshore NW Baltic Sea proper. Mar. Ecol. Prog. Ser. 283, 15.
Højerslev, N., Holt, T., Aarup, T., 1996. Optical measurements in the North Sea-Baltic Sea transition zone. I. On the origin of the deep water in the Kattegat. Cont. Shelf Res. 16, 1329–1342.
Jevrejeva, S., Drabkin, V.V., Kostjukov, J., Lebedev, A.A., Leppäranta, M., Mironov, Y.U., Schmelzer, N., Sztobryn, M., 2004. Baltic Sea ice seasons in the twentieth century. Clim. Res. 25, 217–227.
Kaartokallio, H., 2004. Food web components, and physical and chemical properties of Baltic Sea ice. Mar. Ecol. Prog. Ser. 273, 49–63.
Kahru, M., Nõmmann, S., 1990. The phytoplankton spring bloom in the Baltic Sea in 1985, 1986: multitude of spatio-temporal scales. Cont. Shelf Res. 10, 329–354.
Kahru, M., Elmgren, R., Savchuk, O.P., 2016. Changing seasonality of the Baltic Sea. Biogeosciences 13, 1009–1018.
Kari, E., Kratzer, S., Beltrán-Abaunza, J.M., Harvey, E.T., Vaičiūtė, D., 2016. Retrieval of suspended particulate matter from turbidity – model development, validation, and

application to MERIS data over the Baltic Sea. Int. J. Remote Sens. 38, 1–21.
Khalili, M., 2007. Salt, Water and Nutrient Fluxes to Himmerfjärden Bay. Uppsala University.
Kirk, J.T.O., 2011. Light and Photosynthesis in Aquatic Ecosystems, 3rd ed. Cambridge University Press, Cambridge.
Klais, R., Tamminen, T., Kremp, A., Spilling, K., Olli, K., 2011. Decadal-scale changes of dinoflagellates and diatoms in the anomalous Baltic Sea spring bloom. PLoS One 6 (6), e21567.
Klais, R., Tamminen, T., Kremp, A., Spilling, K., An, B.W., Hajdu, S., Olli, K., 2013. Spring phytoplankton communities shaped by interannual weather variability and dispersal limitation: mechanisms of climate change effects on key coastal primary producers. Limnol. Oceanogr. 58, 753–762.
Kowalczuk, P., Stedmon, C.A., Markager, S., 2006. Modeling absorption by CDOM in the Baltic Sea from season, salinity and chlorophyll. Mar. Chem. 101, 1–11.
Kratzer, S., 2000. Bio-optical Studies of Coastal Waters. University of Wales, Bangor.
Kratzer, S., Moore, G., 2018. Inherent optical properties of the NW Baltic Sea in comparison to other seas and oceans. Remote Sens. 10, 418.
Kratzer, S., Tett, P., 2009. Using bio-optics to investigate the extent of coastal waters: a Swedish case study. Hydrobiologia 629, 169–186.
Kratzer, S., Håkansson, B., Sahlin, C., 2003. Assessing Secchi and photic zone depth in the Baltic Sea from satellite data. Ambio 32, 577–585.
Kratzer, S., Ebert, K., Sørensen, K., 2011. Monitoring the bio-optical state of the Baltic Sea ecosystem with remote sensing and autonomous in situ techniques. In: Central and Eastern European Development Studies (CEEDES). Springer Science + Business Media, pp. 407–435.
Kremp, A., Tamminen, T., Spilling, K., 2008. Dinoflagellate bloom formation in natural assemblages with diatoms: nutrient competition and growth strategies in Baltic spring phytoplankton. Aquat. Microb. Ecol. 50, 181–196.
Lehmann, A., Krauss, W., Hinrichsen, H.H., 2002. Effects of remote and local atmospheric forcing on circulation and upwelling in the Baltic Sea. Tellus A 54, 299–316.
Lei, R., Leppäranta, M., Erm, A., Jaatinen, E., Pärn, O., 2011. Field investigations of apparent optical properties of ice cover in Finnish and Estonian lakes in winter 2009. Estonian J. Earth Sci. 60, 50.
Lenth, R.V., 2016. Least-squares means: the R package lsmeans. J. Stat. Softw. 69, 1–33.
Leppäranta, M., 2003. Investigation of ice and water properties and under-ice light fields in fresh and brackish water bodies. Nord. Hydrol. 34, 245–266.
Leppäranta, M., Myrberg, K., 2009. Physical Oceanography of the Baltic Sea. Springer Berlin Heidelberg.
Lips, I., Rünk, N., Kikas, V., Meerits, A., Lips, U., 2014. High-resolution dynamics of the spring bloom in the Gulf of Finland of the Baltic Sea. J. Mar. Syst. 129, 135–149.
Margalef, R., 1978. Life-forms of phytoplankton as survival alternatives in an unstable environment. Oceanol. Acta 1, 493–509.
McDougall, T.J., Barker, P.M., 2011. Getting started with TEOS-10 and the Gibbs seawater (GSW) oceanographic toolbox. In: SCOR/IAPSO WG127, pp. 28.
Merkouriadi, I., Leppäranta, M., 2014. Long-term analysis of hydrography and sea-ice data in Tvärminne, gulf of Finland, Baltic Sea. Clim. Chang. 124, 849–859.
Merkouriadi, I., Leppäranta, M., 2015. Influence of sea ice on the seasonal variability of hydrography and heat content in Tvärminne, gulf of Finland. Ann. Glaciol. 56, 274–284.
Olenina, I., Hajdu, S., Edler, L., Andersson, A., Wasmund, N., Busch, S., Göbel, J., Gromisz, S., Huseby, S., Huttunen, M., Jaanus, A., Kokkonen, P., Ledaine, I., Niemkiewicz, E., 2006. Biovolumes and size-classes of phytoplankton in the Baltic Sea. Balt. Sea Environ. Proc. 106, 144.
Piiparinen, J., Kuosa, H., Rintala, J.M., 2010. Winter-time ecology in the Bothnian Bay, Baltic Sea: nutrients and algae in fast ice. Polar Biol. 33, 1445–1461.
Pinheiro, J., Bates, D., DebRoy, S., Sarkar, D., Team, R.-C., 2017. nlme: linear and nonlinear mixed effects models. In: R Package Version. 3. pp. 1–131.
Quinn, G.P., Keough, M.J., 2002. Experimental Design and Data Analysis for Biologists. Page Experimental Design and Data Analysis for Biologists. Cambridge University Press.
R Core Team, 2017. R: A Language and Environment for Statistical Computing. R Foundation for Statistical Computing, Vienna, Austria.
Rudstam, L.G., Hansson, S., Johansson, S., Larsson, U., 1992. Dynamics of planktivory in a coastal area of the northern Baltic Sea. Mar. Ecol. Prog. Ser. 80, 159–173.
Seinä, A., Palosuo, E., 1996. The classification of the maximum annual extent of ice cover in the Baltic Sea 1720–1995. In: MERI - Report series of the Finnish Institute of Marine Research. 27. pp. 79–91.
Snoeijs-Leijonmalm, P., Schubert, H., Radziewska, T., Thomas, D.N., Kaartokallio, H., Tedesco, L., Majaneva, M., Piiparinen, J., Eronen-rasimus, E., Rintala, J., Kuosa, H., Blomster, J., Vainio, J., 2017. Biological Oceanography of the Baltic Sea. Page In: Snoeijs-Leijonmalm, P., Schubert, H., Radziewska, T. (Eds.), Biological Oceanography of the Baltic Sea. Springer Science + Business Media.
Spilling, K., 2007. Dense sub-ice bloom of dinoflagellates in the Baltic Sea, potentially limited by high pH. J. Plankton Res. 29, 895–901.
Stipa, T., 2002. Temperature as a passive isopycnal tracer in salty, spiceless oceans. Geophys. Res. Lett 29, 1–4.
STRÅNG, 2017. STRÅNG - a mesoscale model for solar radiation. http://strang.smhi.se/.
Strickland, J.D.H., Parsons, T.R., 1972. A practical handbook of seawater analysis. In: Page A Practical Handbook of Seawater Analysis, 2nd edition. Fisheries Research Board of Canada, Ottawa, Canada.
Thomas, D.N., Dieckmann, G. (Eds.), 2010. Sea Ice, 2nd edition. Blackwell Publishing, Ames, Iowa.
Uotila, P., Vihma, T., Haapala, J., 2015. Atmospheric and oceanic conditions and the extremely low Bothnian Bay sea ice extent in 2014/2015. Geophys. Res. Lett. 1–10.
Uusikivi, J., Ehn, J., Granskog, M.a., 2006. Direct measurements of turbulent momentum, heat and salt fluxes under landfast ice in the Baltic Sea. Ann. Glaciol. 44, 42–46.
Vihma, T., Haapala, J., 2009. Geophysics of sea ice in the Baltic Sea: a review. Prog. Oceanogr. 80, 129–148.
Walve, J., Larsson, U., 2010. Seasonal changes in Baltic Sea seston stoichiometry: the influence of diazotrophic cyanobacteria. Mar. Ecol. Prog. Ser. 407, 13–25.
Warren, S.G., 1982. Optical Properties of Snow.
Wasmund, N., Uhlig, S., 2003. Phytoplankton trends in the Baltic Sea. ICES J. Mar. Sci. 60, 177–186.
Wasmund, N., Nausch, G., Matthaus, W., 1998. Phytoplankton spring blooms in the southern Baltic Sea—spatio-temporal development and long-term trends. J. Plankton Res. 20, 9–117.
Winder, M., Berger, S.A., Lewandowska, A., Aberle, N., Lengfellner, K., Sommer, U., Diehl, S., 2012. Spring phenological responses of marine and freshwater plankton to changing temperature and light conditions. Mar. Biol. 159, 2491–2501.
Zuur, A.F., Ieno, E.N., Walker, N.J., Saveliev, A.A., Smith, G.M., 2009. Mixed Effects Models and Extensions in Ecology with R. Springer Science + Business Media, New York, United States.